COMPARISON OF INTERFACIAL SHEAR STRENGTH MEASUREMENTS FOR BONDED MATERIALS AND COMPOSITE MATERIALS

By

Arun Krishnan

Thesis

Submitted to the Faculty of the

Graduate School of Vanderbilt University

in partial fulfillment of the requirements

for the degree of

MASTER OF SCIENCE

in

Civil Engineering

December, 2008

Nashville, Tennessee

Approved by:

Professor Luoyu R. Xu

Professor Caglar Oskay

To my father, mother and sister

ACKNOWLEDGEMENTS

I would like to acknowledge the contribution of several people who have been influential (and still are) during the course of my graduate study at Vanderbilt. I thank my advisor, Dr. Roy Xu for providing me with academic and financial support. His technical suggestions and eye for finer details have always been of immense help in completing this thesis. Dr. Xu has been a wonderful advisor in that he always encourages one to think and work independently. He has been instrumental in shaping my graduate life. I thank Dr. Oskay for his valuable suggestions and comments in improving my work. I am also grateful to Dr. Basu and Dr. Mahadevan for taking great care and interest in my life and work. Thanks to all my friends in the Civil Engineering department especially to Angel, Liming, Sohini, and Surya for answering my questions and pulling me out of trouble time and again. I should also thank Mr. Zhiao Shi and ACCRE for allowing me access to their servers.

I thank my father for serving as an inspiration and as a role model for all my life, for never letting me down, and for all those wonderful pieces of advice during my times of greatest despair. I thank my mother for always supporting me and making me what I am. Your kind words of encouragement have ever been beneficial. I would have never made it here if not for my parents. Special thanks to my sister as well. You always make me wonder if I am the smaller one. Dad, Mom and Sis, I fully understand your sacrifices and will never let you down. To the three of you I dedicate my thesis.

TABLE OF CONTENTS

LIST OF TABLES

LIST OF FIGURES

CHAPTER 1

INTRODUCTION

1.1 Overview

Composite Materials are made from two or more different types of engineering materials that are combined at a macroscopic scale but behave as one single material. (Kaw, 2006). Individually, materials which find little or limited use, become significantly functional when they are put together. This led to the discovery of composite materials, which found place in almost every historically important civilization. Composites are composed of atleast two types of materials-the reinforcing phase and the matrix. The matrix is the continuous phase in which the reinforcement (which could be fibers, particles or flakes) is embedded. Today, composites have functional relevance in almost every sphere of life, finding applications in such diverse fields as construction of airplane fuselage and wings, ship hulls and bows, domestic items like utensils, glasses, footballs, and at a much smaller scale as nanofillers in dental restoratives. As engineers we need to know how to design, develop, and maintain structures made of composite materials. The universal use of composite materials in today's world brings out the significance involved in determining their mechanical properties. Since composites are made of two or more materials, there always exists an interface between the different types of material components. This interface could be in the form of mechanical or chemical bonding between the different components. However, in general the interface usually becomes the weakest link in a material due to the shift in properties across this region. This makes the

interface prone to failure. Hence it becomes necessary to investigate and characterize interfacial properties.

Shear is a major mode of failure in composite materials. The shear behavior of several composites becomes dependent on material orientation, thereby making them more susceptible to failure in this mode. Systematic experimental investigations by Xu and Rosakis (2002) have shown that shear-dominated delamination is a major dynamic failure mode in layered sandwich structures. In the same work, the authors conclude that inter-layer crack growth, under certain conditions, precedes other modes of failure such as intra-layer or core cracking. In Fig. 1.1, it can be seen that under the impact of a projectile, a model sandwich composite structure tends to fail in shear by delamination at the interface between the layers. The shear dominated cracks also dictate the further failure of the structure depending on factors such as crack speed, specimen geometry (free edge effects at bi-material corners) and inter layer shear stress. (Xu and Rosakis, 2002). Thus, the interfacial shear strength becomes an important criterion determining how and when a composite material will fail. It becomes a key property for any new composite material. Evaluating the interfacial strength has become crucial for determining the strength, durability and performance of modern composite materials. Naval and airplane structures use a large percentage of composites in their structural design. In such structures, understanding the shear behavior becomes all the more important due to the significance of the structure involved.

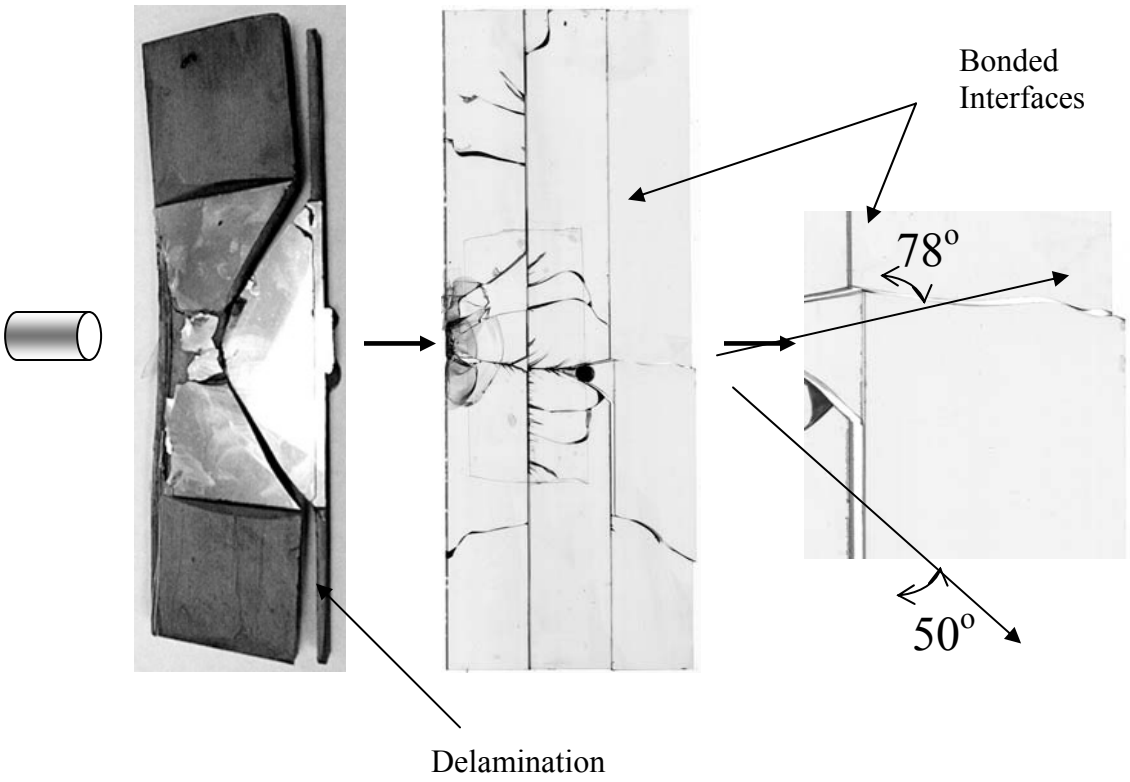

(a) Real Sandwich **(b) Model Sandwich** **(c) Failure Mode**

Fig. 1.1 Shear Dominated delamination is a major dynamic failure mode of layered sandwich structures (from Xu and Rosakis, 2002)

However, the shear at the interface is often a complicated property to estimate, as it rarely shows uniformity across the interfacial region. This could be due to the presence of stress singularities at sharp corners and material interfaces (Bogy, 1971). Also, when two different types of materials are bonded together, there is always a stiffness mismatch due to difference in elastic moduli causing stress singularities at bi-material corners and edges. The presence of a weak adhesive layer at the interface only compounds the problem. In case of dissimilar materials, there exists a stress singularity at the interface and the asymptotic stress field can be expressed as

$$\sigma_{ij} \sim r^{-\lambda} f_{ij}(\theta) \tag{1.1}$$

Here λ is the stress singularity order, which should be minimized to reduce the effect of the stress singularity. It is seen that the stress is proportional to a negative power of λ and hence shoots up close to the tip of the singularity. The stresses in a two edge-bonded elastic wedges of different materials and wedge angles under surface tractions have been analyzed (Bogy, 1971).

$$f(\theta_1, \theta_2, \alpha, \beta, p) = A\beta^2 + 2B\alpha\beta + C\alpha^2 + 2D\beta + 2E\alpha + F = 0 \qquad (1.2)$$
$$p = 1 - \lambda$$

where A to F are functions of the wedge angles theta 1 and theta 2 and are expressed in terms of an auxiliary function. For a particular combination of wedge angles the stress singularity order can be estimated. Inversely, for a given stress singularity order, the wedge angles can be estimated. This allows for the design of appropriate specimens with reduced effect of stress singularities. (Sreeparna, 2007) A similar approach has been used in the present work to design the specimen dimensions and notch angles. A value of 45 degrees is used for the notch angles in this case to reduce the order of the stress singularities.

Also, the shear strength of any material is a difficult property to estimate unlike the compressive or tensile strength where a simple tension or compression test becomes sufficient. Since shear cannot be measured directly, several indirect methods have to be used. A preferable and logical requirement of any shear test would be the presence of a region of uniform shear in the zone where the shear is being measured. During the past several decades, extensive work has been done for the experimental identification of shear properties in materials. Different shear methods of testing including the Iosipescu

shear test and the off-axis tensile test have been proposed. The Iosipescu test which is of interest in this thesis, was first developed by a Romanian scientist of the same name in order to measure the shear strength of metal rods (Iosipescu, 1967). Though not the ideal shear test, it has been satisfactory and has been used in its modified form to measure the shear strength of composites over the past several years. Comparisons between the different methods of testing have indicated that the Iosipescu test has a slight advantage over other tests when it comes to measuring properties of composites (Xavier et al., 2004). The Iosipescu shear test has been studied extensively with the current fixture being developed by Walrath and Adams in the early eighties. The test has also been modeled numerically using finite elements and extensive research has been carried out on failure properties, specimen and fixture design, and applicability to different types of materials. However, the Iosipescu specimen and fixture require machining in a specific pattern that would lead to greater costs and time. The entire process including specimen design and preparation, experimental set-up and testing requires great expertise, time and increased cost and cannot be performed by a layman. This leads to the question: Is such a specialized and complicated test required for estimating a simple and basic material property namely shear strength? Though previous literature and works over the years have looked into almost every aspect of the Iosipescu shear test, they fail to address the basic question posed above. The Iosipescu test has always been accepted as a satisfactory testing procedure despite the complications involved in testing, cost and time for preparation. The purpose of this thesis is to conduct systematic experimental and numerical investigations with an aim to address the issue regarding the need for Iosipescu shear test. By studying and understanding the non-linear variation of shear stress across

the interface, this thesis attempts to provide answers to the need of the Iosipescu shear test.

1.2 Objectives

The objective of this study is to present an integrated experimental and numerical analysis of shear specimens and to analyze the effect of non-linear stress distribution at the interface of shear specimens. As mentioned in the previous section, the Iosipescu test raises questions about its credibility as a shear test for composites. It is not clear if this sort of a specialized test would be required for testing composite materials in everyday life. Chapter 2 describes experiments used to measure the shear strength of material. Two types of specimens, as explained in the next chapter, are used to assist in bringing out the difference. Photoelastic materials are used in order to generate fringe patterns of shear stress and these are recorded using visual means to provide for better understanding of the failure process. A finite element model of the specimen is constructed and the loading procedure is simulated to obtain numerical fringe patterns. The latter is used for validating the numerical simulations after comparisons with the experimental fringe patterns. This is explained in detail in Chapter 3. Finally in Chapter 4, a Monte Carlo simulation is utilized to understand the failure process. Crack length and crack location along the interface are varied to obtain an output distribution of shear stress. Detailed assumptions and results are presented in Chapter 4. Finally conclusions are drawn commenting on the efficacy of the Iosipescu test using data from the analysis of the non-linear shear stress across the interface of the shear specimens.

CHAPTER II

EXPERIMENTAL INVESTIGATION OF THE IOSIPESCU AND BUTT SHEAR SPECIMENS

2.1 Introduction

2.1.1 Overview of Iosipescu and Butt-shear specimens

The Iosipescu test was developed by a Romanian scientist of the same name as a new method for testing shear in metal rods. (Iosipescu, 1971) This test differs from other shear tests in that it provides a zone of uniform shear in the testing zone. In this chapter, an experimental investigation of two types of shear specimens, namely the Iosipescu and Butt-joint shear specimen, is carried out and the results are presented. The results provide a basis for understanding the non-linear shear behavior at the interface of these two types of specimens in order to allow for a better comparison.

The Iosipescu test is an in-plane shear test used for the testing of composite materials. This test makes use of a notched specimen (Iosipescu specimen) loaded in such a way that the total bending moment on the sample is zero and the shear stress across the interface is fairly uniform. A butt-joint shear specimen on the other hand does not have the notch and thus is straight edged at the interface of failure. Now, it is also possible to test a butt-shear specimen using the Iosipescu fixture (also known as modified Walrath fixture after modifications to the existing fixture by Walrath and Adams, 1980). The two specimens have similar dimensions and the only variation is at the interface where the Iosipescu specimen differs in having the V-shaped notch. The variation of the shear stress

across the interfaces of the Iosipescu and Butt-shear specimens along with the specimens themselves are shown in Fig. 2.1. It is seen that the variation of shear stress across the interface of the butt-shear specimen is parabolic as is expected from basic mechanics of materials approach. This is seen as unfavorable for a shear test (Tarnopol'skii et al., 2000) due to absence of a constant magnitude of shear lending suspicion to the value of the measured strength. The Iosipescu specimen, on the other hand, shows a near constant variation of interfacial shear stress seemingly favorable for a shear test. It should be noted that in our case, bonded specimens are tested as opposed to monolithic specimens. The shear stress distribution however would be the same at the interface which would be determined by the loading pattern in case of monolithic specimens. The latter has been discussed elsewhere (Sreeparna, 2007) in detail. The near uniform variation of shear stress is seen as a major advantage of the Iosipescu test over other types of shear tests.

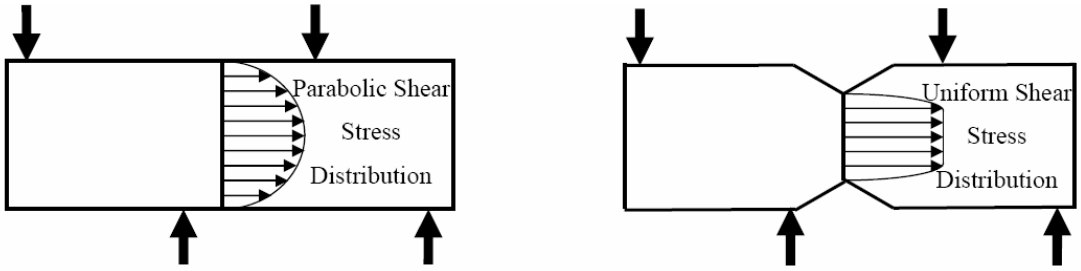

Fig. 2.1 Comparison of the shear stress across the interface of Butt-shear specimen and Iosipescu specimen

In this experimental investigation, these two types of shear specimens are subjected to mechanical testing using the Iosipescu fixture in order to determine their shear strengths. Photoelastic fringe patterns are generated using experimental techniques and are used for the validation of the finite element model.

2.2 Experimental Investigation

2.2.1 Test Materials and Specimens

Test specimens were made of three different types of materials including Aluminum, Polymethyl methacrylate (PMMA) and Polycarbonate. These were utilized in making butt-joint type specimens and Iosipescu specimens as shown in Fig. 2.1. The specimens were not monolithic but were bonded from individual halves. The reason for bonding is that the shear specimens should fail at the interface by shear and not in tension at the upper edges. Previous works have shown failure at the upper edges in tension which would become undesirable in this experiment. Loctite 384 was used as the interfacial bonding adhesive. One of the key requirements in choosing the adhesive was that its strength should be close to or lesser than that of the bulk material. If the strength of the adhesive were more than that of the bulk material, then the specimen would not fail in shear and would fail in some other mode which would become undesirable. The adhesive properties were chosen to be close to those of the bulk polymers in order to minimize the stiffness mismatch. Also, this eliminates the need for modeling the adhesive interface. It is very difficult to estimate the nature and thickness of the adhesive layer and in choosing an adhesive having properties close to that of the bulk material, the need for modeling adhesive failure in the specimen is effectively eliminated.

Individual specimens have a total length of 76.2 mm (each half is 38.1 mm in length) and have a width of 19.1 mm in case of butt-joint shear specimens and 11.4 mm in case of Iosipescu shear specimens. The specimen thickness slightly varied depending on the type of material used. The thickness was 5.4 mm in case of Polycarbonate

specimens and 6 mm in case of Aluminum specimens. The specimens were bonded using a fixture to guarantee their dimensionality even after they were bonded. The individual halves were machined to ensure that they were of the desired dimensions and were sand-blasted at the bonding surfaces to provide for good adhesion. The specimens were left to cure for a period of about 24 hours after they were bonded. It was important to ensure that the adhesive layer was of negligible thickness as otherwise this would interfere with the shear behavior of the specimen. The optimum thickness of the adhesive layer should be less than 20 μm. Some of the specimens where the adhesive layer was visible to the eye or where the bonding was not of good quality were rejected. The results from the experimental investigation were recorded and are reported in a later section.

2.2.2 Experimental Setup

The test set-up consists of three parts including a mechanical system for testing the specimens, an optical system used to develop fringe patterns and an imaging system to capture and record the images. A schematic diagram of the set-up is shown in Fig. 2.2. The mechanical testing system included an MTS 810 test machine and an Iosipescu test fixture. The Iosipescu fixture (Modified Walrath fixture) was mounted on the loading plates of the MTS test machine and the load was transferred using a loading cell. The individual specimens (both butt-joint and V-notched) are mounted on the Iosipescu fixture as shown in Fig. 2.3. It can be seen that Iosipescu fixture has a fixed left part and a movable right part. The movable part is connected to the MTS system whereas the left end is held fixed. The applied load, thus shears off the specimen at the interface. The screws on each part have to be tightened to ensure that the load is transmitted to the

specimen. It should be noted that due to the various parts involved, there will be energy losses due to friction and hence the measured value will be different from the actual value. This difference though would be minimal if the experiment is set up with necessary care. It is interesting to note that the blocks applying the load to the specimen do not extend for the entire length of the specimen. However, they are anti-symmetrically placed. This condition becomes important when the loading condition is simulated and is explained in greater detail in Chapter 3.

The optical system was used to capture the fringe patterns that were generated while loading the specimens. The optical system consists of a laser source (He-Ne laser source, 17 mW) which generates a laser beam collimated using a laser collimator. Circular polarizers and a convex lens are used to further reduce the intensity of the laser beam and to assist in capturing the fringe patterns. The fringe patterns developed only in case of the transparent specimens and the photoelasticity experiment was not carried out on the aluminum specimens. The isochromatic fringe patterns observed are the contours of the maximum in-plane shear stress and are given by the formula

$$\tau_{\max} = \frac{(\sigma_1 - \sigma_2)}{2} = \frac{Nf_\sigma}{2h} \quad , \tag{2.1}$$

where σ_1 and σ_2 are the in-plane principal stresses, N is the fringe order, f_σ is the stress-fringe constant, and h is the thickness of the specimen. (Stress-fringe constant for Polycarbonate is 7 KN/m/fringe). The function of the collimator was to provide a large and collimated laser beam (diameter of 50 mm), since the field of view of our specimens was at least 10 mm. The purpose of the mirror was to adjust the laser beam to the desired position for a specific experiment. The imaging system included a high-resolution digital camera to capture the fringe development and a density filter in front of the camera to

reduce the laser intensity since the laser beam enters the camera directly. Because the laser beam diameter was about 50 mm, a convex lens (focal length of 150 mm) was added to the system to record the whole image. An important issue in obtaining good-quality photos is that the digital camera must be focused at infinity, and the distance between the convex lens and the specimen should be slightly larger than the focal length of the convex lens. Further, the specimens being tested for photoelasticity had a red circular marker of 0.75" diameter (as seen in Fig. 2.3). This marker is used for identifying the dimensions of the specimens in the fringe pattern pictures and is seen as a dark black circle in the experimental fringe pictures.

The Iosipescu test fixture was used in the mechanical loading assembly as described above. The load was applied in the form of displacement at a rate of 1 mm/min. The failure load was recorded and the load-displacement curve for each specimen was obtained. About 30-40 specimens of each type (Iosipescu and Butt-shear) were tested for each material type in order to ensure repeatability. Almost all of the specimens failed due to shear at the interface and not in any other mode which was necessary in this case as we are measuring the shear properties. Pictures of the fringe patterns at various loads were taken and videos depicting the development of fringes from the beginning of loading till failure were recorded.

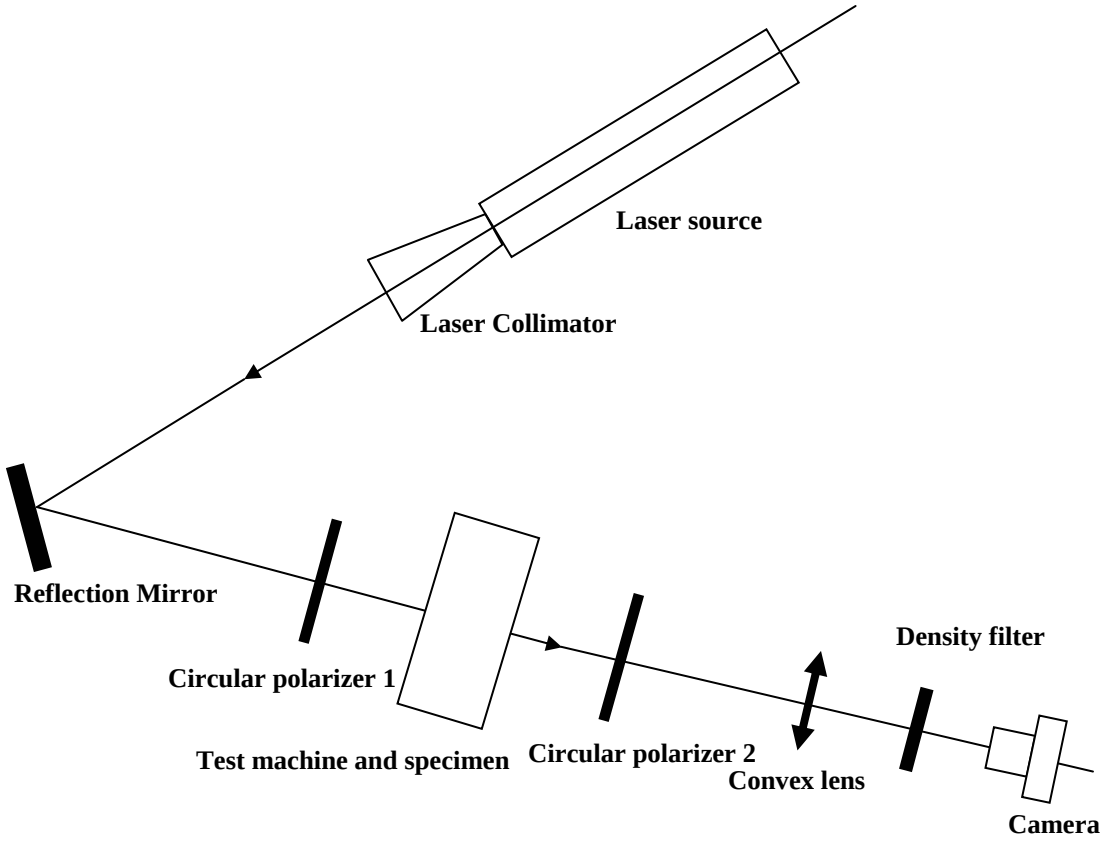

Fig. 2.2 Schematic diagram of the experimental setup used to test the Iosipescu and Butt-shear specimen

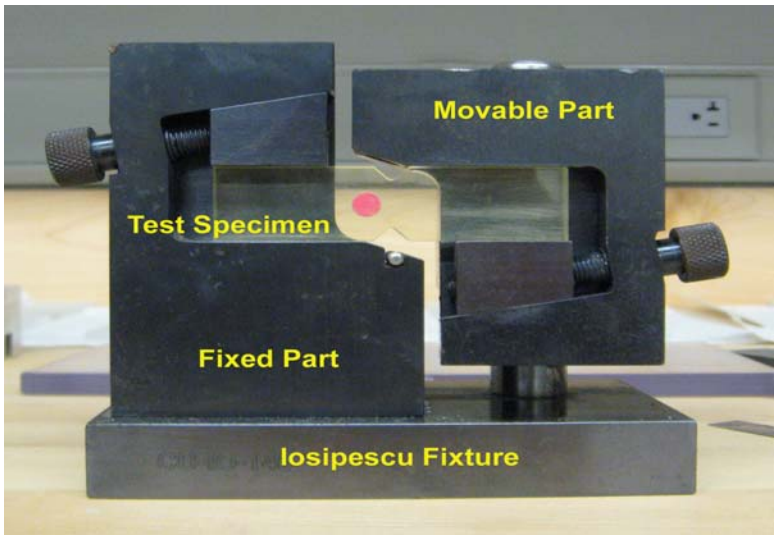

Fig. 2.3 Iosipescu fixture with the mounted Iosipescu V-notch specimen.

2.3 Results of the Experimental Investigation

In this section the results from the experimental investigation of the shear specimens are discussed. The shear strength at the interface was measured for each of the specimens and was recorded as shown in Table 2.1. It should be noted that the failure in all of the specimens was sudden and brittle. Also, the failure occurred in shear and no tensile failure was observed by cracking at the upper edges.

Table 2.1. Measured Bonding Strength Data

SPECIMEN TYPE	IOSIPESCU SHEAR	BUTT-JOINT SHEAR	DIFFERENCE (in %)
	In MPa	In MPa	
Aluminum-Aluminum	10.75 +/- 2.39	10.16 +/- 2.41	**5.5 %**
Polycarbonate-Polycarbonate	10.99 +/- 1.45	8.51 +/- 1.13	**22.5 %**
PMMA-PMMA	11.58 +/- 2.15	10.19 +/- 0.57	**12 %**

The above table presents the measured bonding strength data of our experimental tests. The first column reports the strength data for Iosipescu specimens and the second column presents the same for butt-joint shear specimens. The mean and the standard deviation values are reported in Mpa. The third column shows the difference in the values of mean shear strengths between the two types of shear specimens.

From the above table it is seen that the average values are close to that of the shear strength of the interfacial adhesive indicating that most of the specimens have failed in shear. The means and standard deviations of the Iosipescu and Butt-shear specimens for the three different types of materials are presented in Table 1. The

covariance values are not too high indicating the repeatability of the experiments. In case of the Butt joint shear specimens, the covariance value tends to be a little higher in comparison with the Iosipescu specimens. This is due to the presence of a greater degree uniform shear stress across the cross section of the Iosipescu specimen. But even otherwise, the covariance values are below 23% in all cases and are acceptable. The difference between the bonding strength of the Iosipescu and Butt-shear specimens is also shown here. The Iosipescu specimen shows a greater value of measured bonding strength in all the three types of material used here. This is because of the lower cross sectional area of the Iosipescu specimen at the interface. The Iosipescu specimen has about 60% of the cross sectional area of the Butt-joint shear specimen. The difference in shear strengths in case of Aluminum specimens is only 5.5 %, and in case of PMMA is 12%. Even for Polycarbonate specimens, the difference in values is only 22%, which would be an acceptable value. The load-displacement values are also recorded for every specimen. This curve is almost linear until failure when the specimen undergoes brittle failure. There is an initial gap between the specimen and fixture which causes a small non-linear part in the diagram, but this has nothing to do with the material properties. A similar load-displacement plot is obtained for all the three types of materials and specimens.

The histograms of the measured data are also shown in Figs 2.4 for PMMA specimens, Fig. 2.5 for Aluminum specimens and Fig. 2.6 for Polycarbonate specimens. The histograms also indicate a normal curve which is fitted in order to allow for a better visualization. It should be noted that the histograms for each type of material is plotted on the same scale to give a fair comparison. From Fig. 2.4 for PMMA specimens it is observed that Iosipescu specimens show a greater spread in comparison with their Butt-

shear counterparts. However, the means remain more or less same and the difference is only 12% in the means (from Table 2.1) compared to the difference in standard deviations which is close to 75%. The butt-joint shear specimens show a greater spread in all cases. This can be accounted for by the difference in cross sectional areas. Since Iosipescu specimens have a smaller cross section at the interface, the possibility of a larger flaw occurring is significantly reduced compared to the butt-joint shear specimen. It should be noted that even the in case of butt-joint specimens, the standard deviations is not significantly high. However, the difference between the means is lesser compared to the difference between the standard deviations. This seriously undermines the need for the Iosipescu shear test. If the mean values are similar, and only the standard deviations differ, a butt-joint shear specimen might very well replace the specialized Iosipescu specimen.

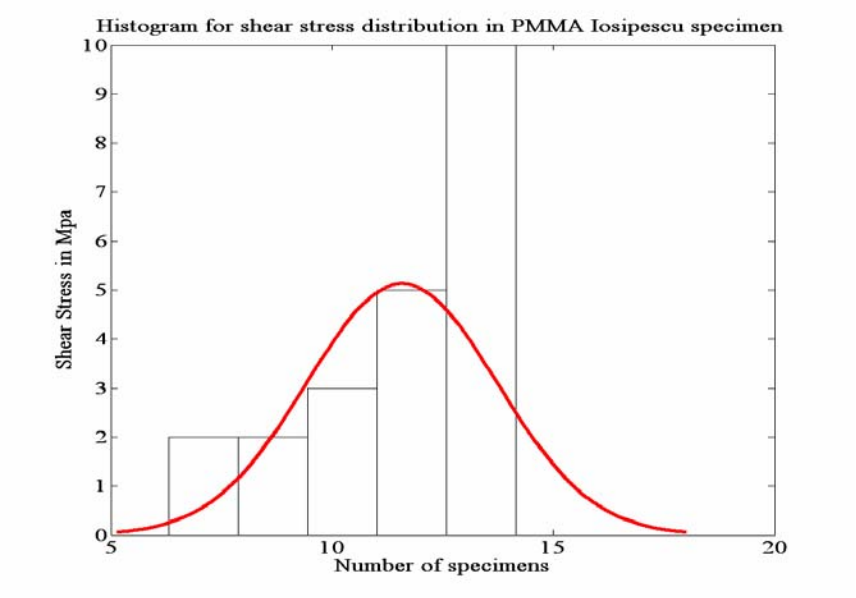

(a)

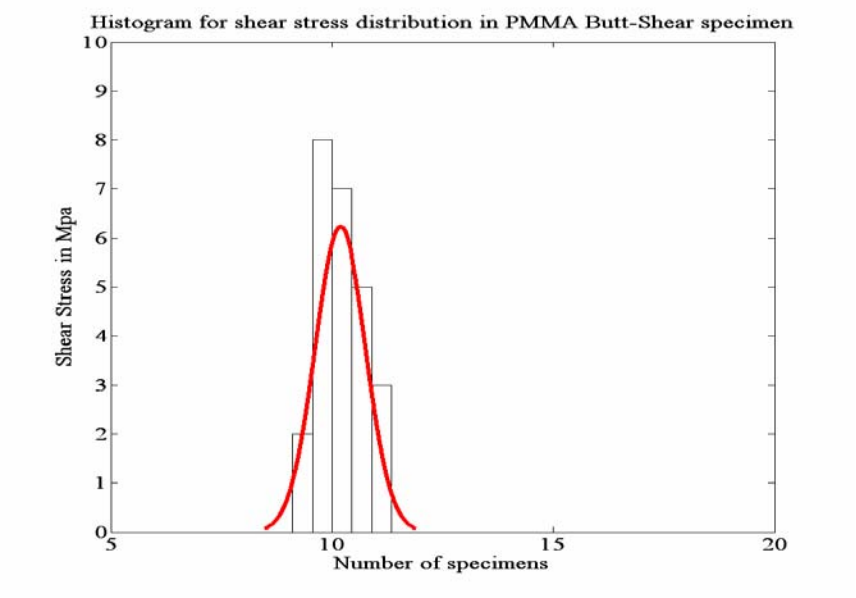

(b)

Fig 2.4 Comparison of the experimental histograms of measured bonding strength data of PMMA specimens for (a) Iosipescu specimen (b) Butt-shear specimen

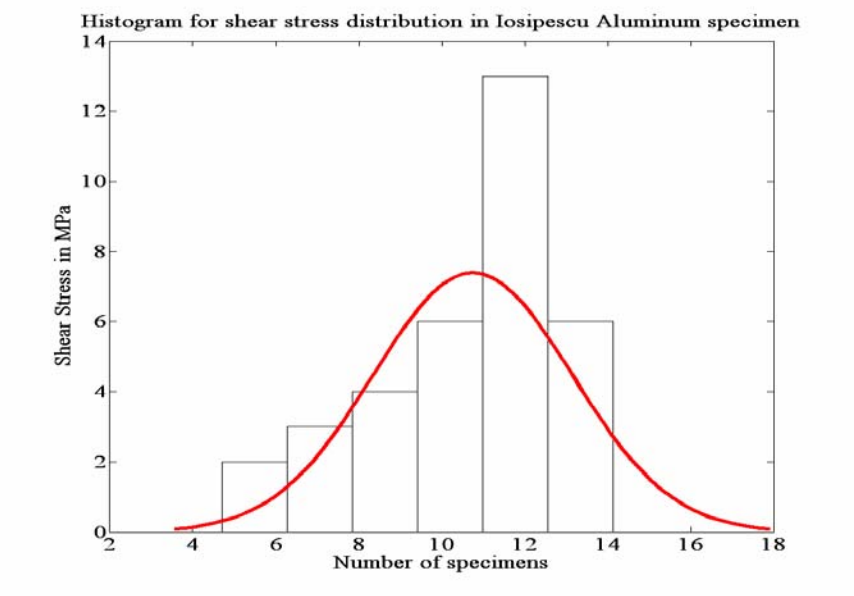

(a)

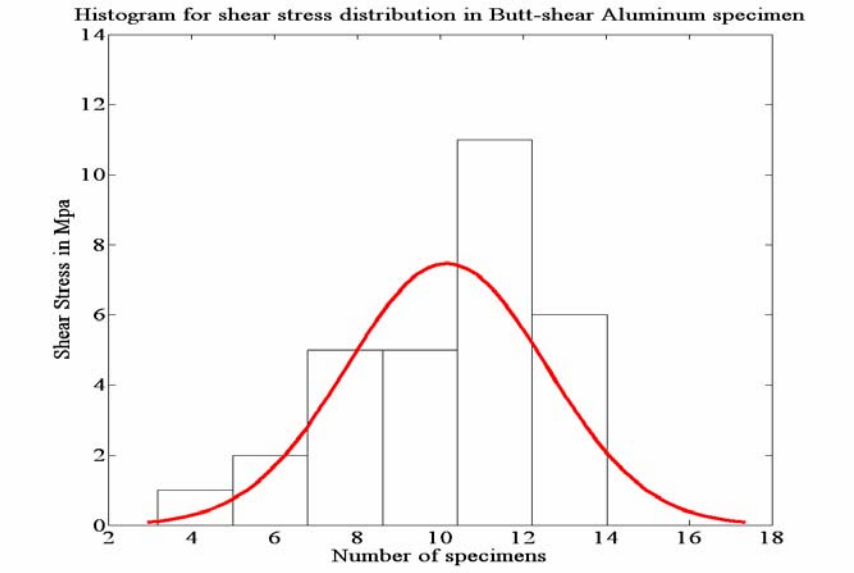

(b)

Fig 2.5 Comparison of the experimental histograms of measured bonding strength data of Aluminum specimens for (a) Iosipescu specimen (b) Butt-shear specimen

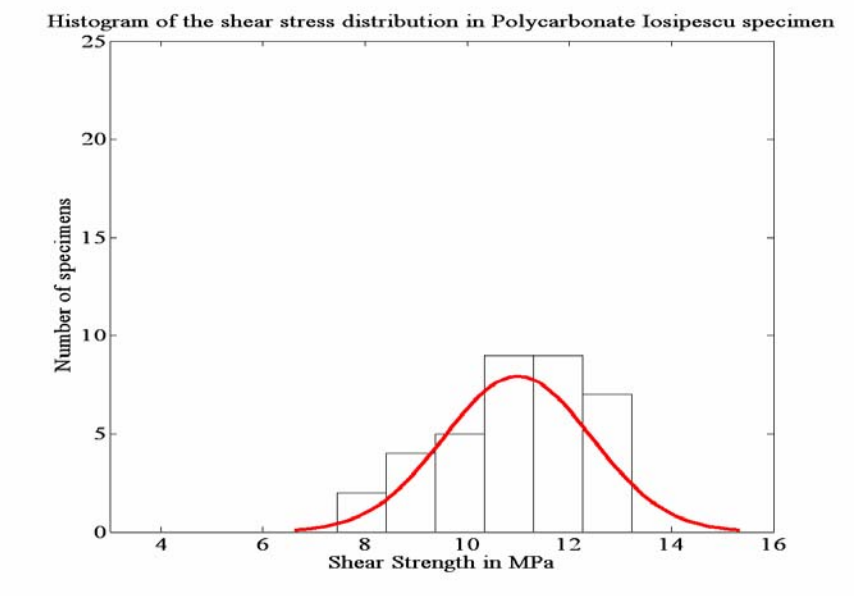

(a)

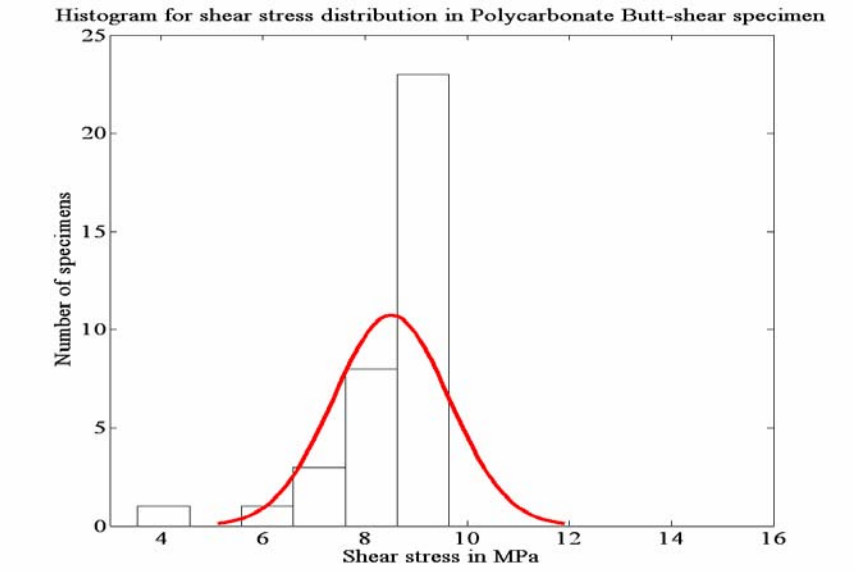

(b)

Fig 2.6 Comparison of the experimental histograms of measured bonding strength data of Polycarbonate specimens for (a) Iosipescu specimen (b) Butt-shear specimen

CHAPTER III

FINITE ELEMENT MODELING AND NUMERICAL SIMULATION OF FRINGE PATTERNS

3.1 Finite Element Modeling of shear specimens

3.1.1 Modeling of the shear specimens

A finite element model of the specimen was built using the popular finite element software ANSYS 11.0 to obtain the distribution of the stresses in the specimen. It becomes sufficient to consider the finite element model of the bulk specimen as opposed to the bonded specimen. The rationale is as follows: we are comparing the fringe patterns of the shear specimens at a loading which is much lower than the failure load. The stress transfer across the interface will remain as though the specimen were monolithic and not bonded as can be seen from our experimental fringe patterns in Fig. 3.3 and Fig. 3.4. Hence a monolithic finite element model would be sufficient for comparing the fringe patterns. However, it should also be noted that during our experiments we make sure that the thickness of the adhesive layer remains relatively negligible compared to the dimensions of the specimen.

The stress and strain fields of the bonded specimens were analyzed using the commercial finite element software ANSYS. A two dimensional analysis was considered as the stress variation in the other directions is negligible. Two different types of materials were chosen to represent the actual experiment. The materials chosen were Polycarbonate with an Elastic Modulus of 2.4 Gpa and a Poisson’s Ratio of 0.35 and

Aluminum with an Elastic modulus of 70 Gpa and a Poisson's ratio of 0.35. A linear, elastic and isotropic material was chosen as only brittle materials are considered in this analysis. The dimensions of the specimen were: width of 76.2 mm (individual parts have a width of 38.1mm) and a height of 20 mm. Since we only consider a two-dimensional analysis, the thickness of the specimen was chosen as 1 mm. A plane stress analysis was adopted. The above dimensions were chosen to represent the actual specimen used in experiments. The notch angle was chosen as 90 degrees in order to reduce the effect of stress singularities. The notch depth was 3.8 mm. The specimen was meshed using Plane 42 quad elements. A finer mesh was used in the notch region in order to capture any stress singularities. A coarser mesh was used elsewhere to save on computational time and effort. Plane 42 elements were exclusively used in order to meet to meet the requirements of the plotting software Tecplot. A plot of the mesh used in the actual analysis is shown in Fig. 3.1.

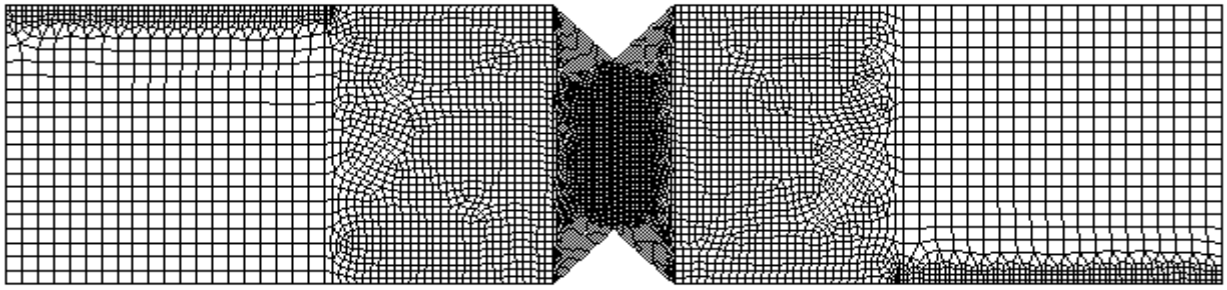

(a)

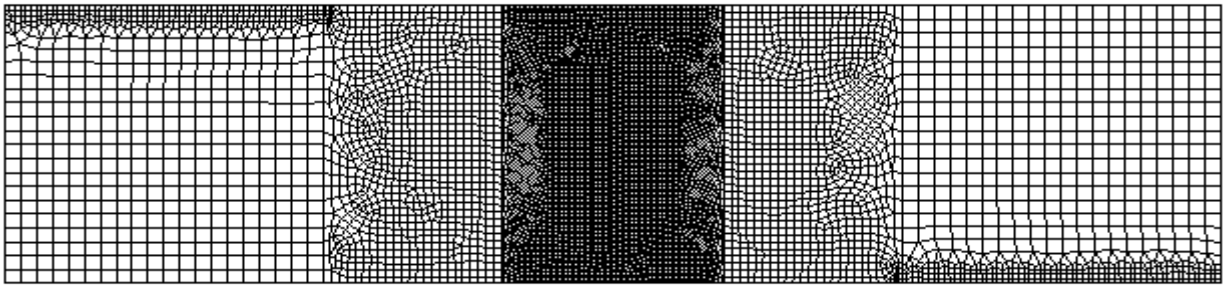

(b)

Fig. 3.1 Finite element mesh used for modeling the (a) Iosipescu specimen and (b) Butt-shear specimen

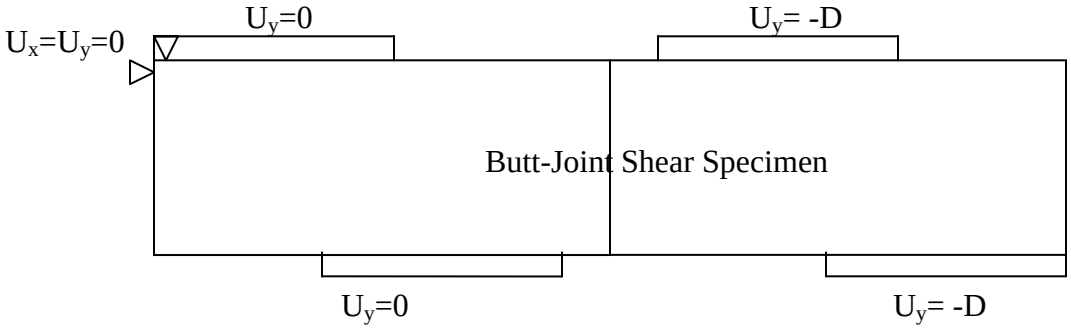

Fig. 3.2 A Schematic diagram showing the transfer of boundary conditions to the finite element model

3.1.2 Modeling of the boundary conditions

Even though a considerable amount of numerical research has been done on the Iosipescu specimen, there has been a lack of consensus on representing the boundary conditions. (Ho et al.,1992). Uniformly applied loads (Barnes et al.) and concentrated forces (Sullivan et al.) have been used earlier. However, the non-linearity of the problem implies that it would be very difficult to obtain a correct distribution of the load on the loading blocks. Thus, it becomes necessary to apply the load in the form of displacements. This is also a better simulation of the experimental investigation as the loading was done by displacement control. The procedure for simulating the boundary conditions was adopted similar to the one mentioned in Kumosa et al. A schematic diagram of the transfer of boundary conditions to the model is indicated in Fig. 3.2.

A linear static analysis was adopted in order to simulate realistic load transfer from the fixture to the specimen. In order to incorporate a realistic simulation of the load transfer from the fixture to the specimen, an iterative procedure was adopted. Since the load distribution on the edges is highly non-linear and cannot be estimated, the load was applied in the form of displacements. The left portion of the specimen is fixed and cannot move in the vertical dimension. Displacement constraints are applied similar to what is observed in reality. The top left edge node is restrained from moving in both x and y directions in order to prevent rigid body movements. On the right portion, an initial vertical uniform displacement is applied. Now the reaction loads at each of the nodes with a constraint is checked to verify that they are not in tension. The constraint was removed from those nodes which showed a tensile reaction force instead of a compressive one and a new analysis with the updated set of boundary conditions was

carried out. This was done until convergence and the total applied load was obtained by integrating the shear stress across the interface of the specimen. The load applied in the form of displacements was initially obtained from the experimental load-displacement plot. The actual load on the specimen was later obtained by integrating the shear stress along the interface. This procedure was iteratively carried until the required load (for matching the fringe patterns) was obtained. A small tolerance of not more than 5 % was used here. It should be noted that the experimental fringe pattern is not at the exact load which is mentioned as there will be a slight time difference between the time the load reading is taken and the time the photograph is obtained. Thus, this tolerance is justified.

3.1.3 Photoelastic fringe plots

The numerical photoelasticity plots were obtained by plotting the stress distribution after the convergence of the finite element analysis using the plotting software Tecplot. The maximum shear stress was obtained from the numerical analysis by using the principal stress values. This was then converted to a fringe number N which in turn was converted into a grayscale value. Half order fringes (0.5, 1.5, 2.5, etc.) were given a value of 255 and full order fringes (0, 1, 2, etc.) were assigned a value of 0 on the grayscale spectrum. The fringe patterns that are obtained are contours of the maximum in-plane shear stress.

3.2 Validation of the numerical analysis

3.2.1 Comparison of the photoelastic fringe patterns

The numerical modeling of the shear specimens was validated by comparison of the numerical photoelastic fringe plots with the experimental ones. The comparison for Iosipescu specimens is shown in Fig. 3.3 and a similar comparison for the butt-shear specimens is shown in Fig. 3.4. It is seen that the experimental and numerical patterns have a pretty close match. The fringes appear concentrated around the top and bottom loading blocks. This is due to the highly non-linear force distribution on the upper right and lower left loading blocks. As the loading is anti-symmetric, similar load distributions are obtained on these two blocks. The number of fringes increase as the loading is increased. A video of the development of the fringes was also obtained from initial loading till failure of the specimens. It should be noted that the fringes remain continuous across the interface in most of the experimental pictures. The scaling mark appears as a dark circle in the experimental pictures whereas it is absent in the numerically simulated pictures.

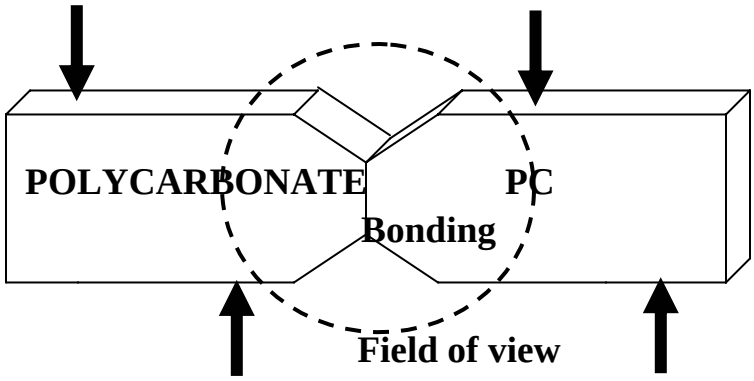

EXPERIMENTAL **SIMULATED**

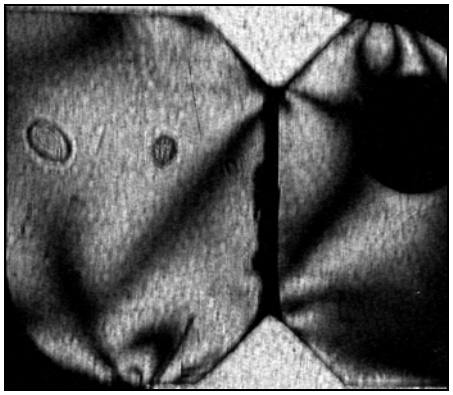

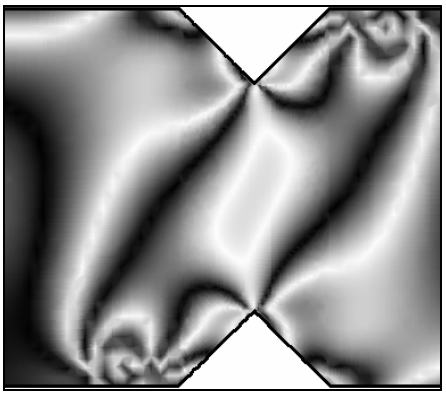

(a) **Applied Load = 100 +/- 5 N** (b)

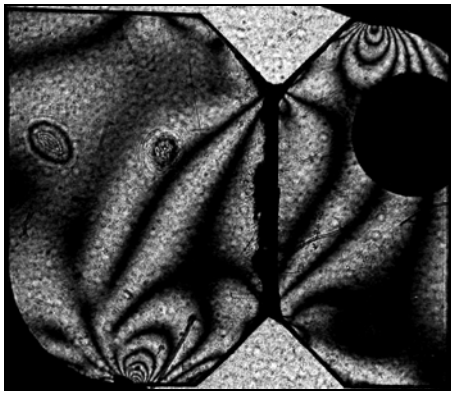

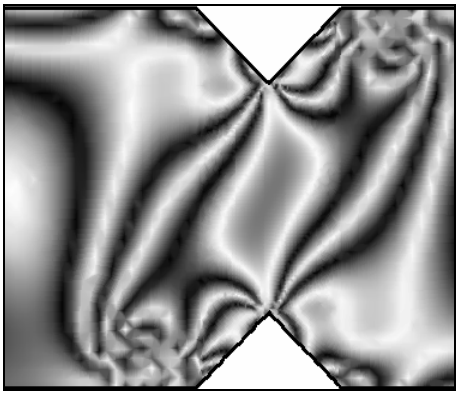

(c) **Applied Load = 200 +/- 5 N** (d)

Fig. 3.3 Comparison between experimental and finite element generated fringe patterns for Iosipescu specimen made of Polycarbonate

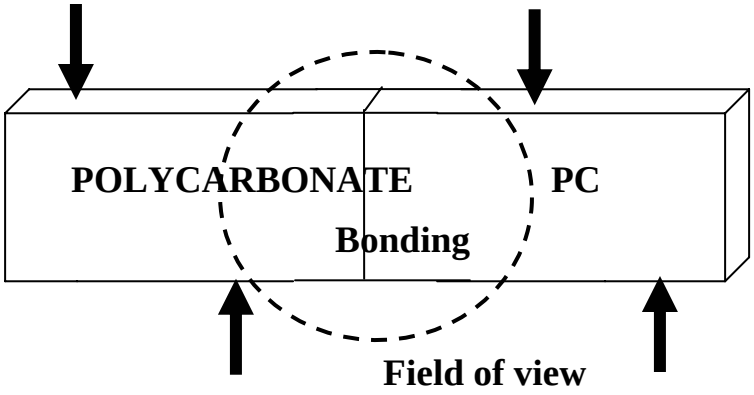

EXPERIMENTAL **SIMULATED**

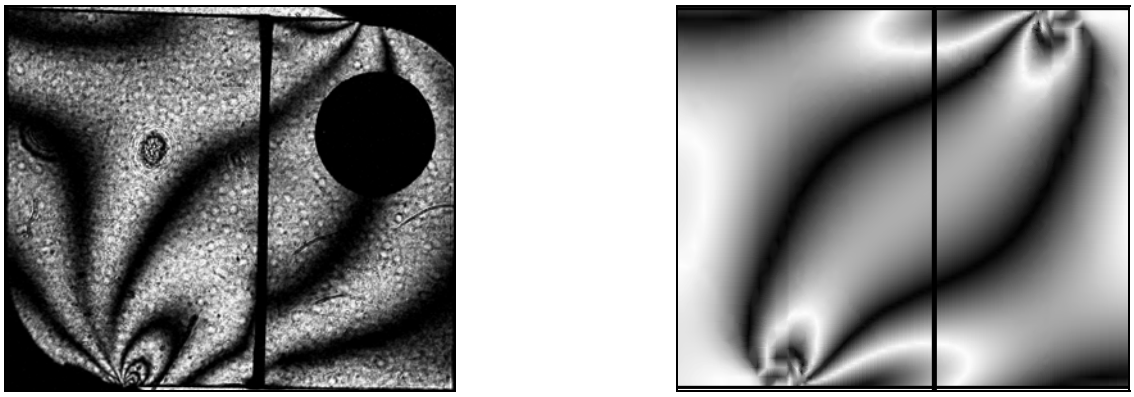

(a) **Applied Load = 100 +/- 5 N** (b)

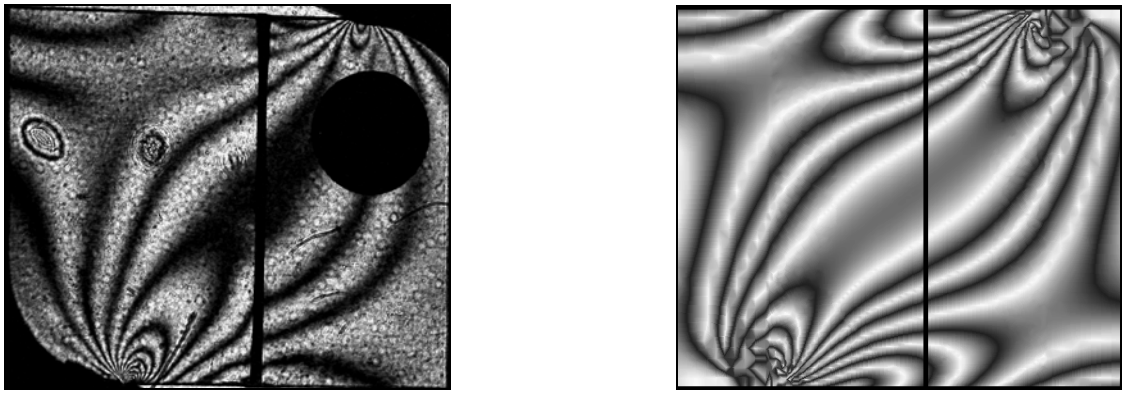

(c) **Applied Load = 200 +/- 5 N** (d)

Fig 3.4 Comparison between experimental and finite element generated fringe patterns for Butt-joint specimen made of Polycarbonate

3.2.2 Fair comparison of the interfacial shear stress

Since different cross sectional areas are involved in our experiments, the same average stress level has to be used at the interface to obtain a fair comparison of shear stress. Thus, an Iosipescu and a butt-shear finite element model having the same cross sectional area is utilized in the numerical modeling before the same load is applied. This variation in shear stress at the interface is as shown in Fig. 3.5. It can be seen that the variation in shear stress at the interface is parabolic for the butt-shear specimen, but almost constant for the Iosipescu specimen. Also, upon integration, the same load will be obtained which allows for a fair comparison.

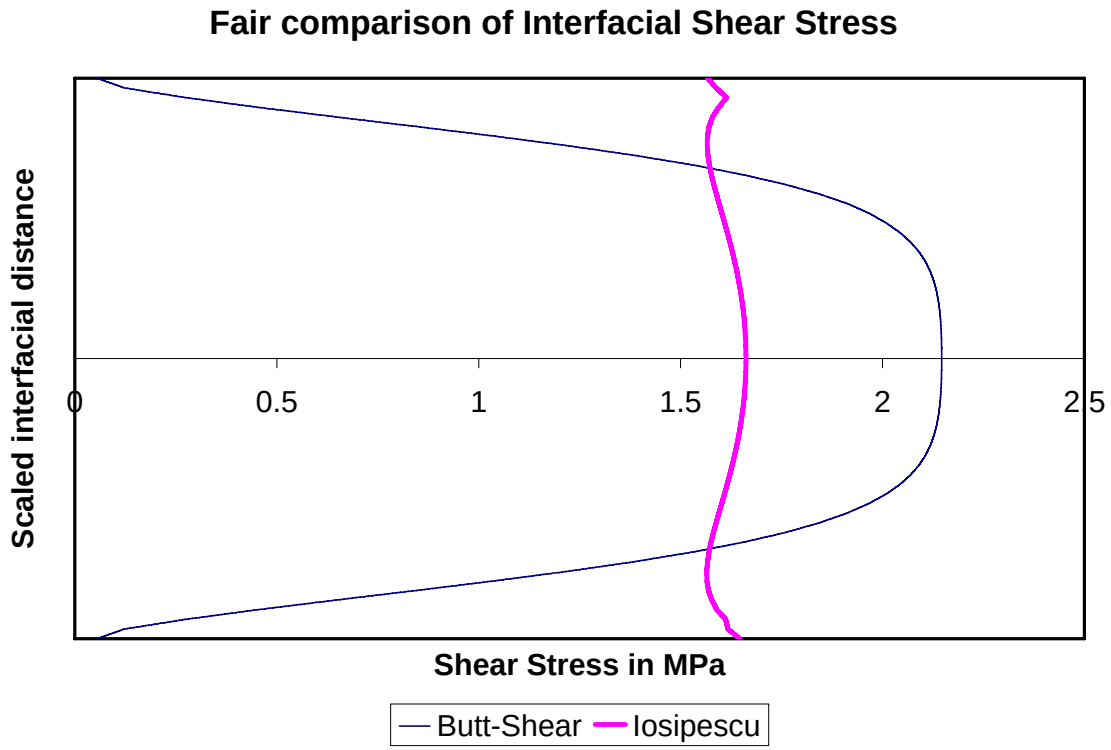

Fig. 3.5 Comparison of shear stress at the interface between Butt-shear specimen and Iosipescu specimen.

3.2.3 Investigation into the quality of bonding at interface

An error analysis to investigate the effect of improper bonding was carried out. Since the bonding was done manually, errors are expected in workmanship which will lead to dimensional inaccuracies. In order to investigate the effect of this on the shear strength at the interface, finite element models with small offset of the individual halves at the interface was built and a similar analysis was carried. The distribution of shear stresses at the interface was compared to the ideal model and the difference was found to be negligible. This confirms that the difference between our experimental specimens and numerical models will be less. Although in the numerical simulations an ideal model is used, in reality this model becomes impossible to construct. However, the difference in shear distributions at the interface is minimal which reassures our faith in the experimental specimens.

CHAPTER IV

MONTE CARLO SIMULATION FOR INTERFACIAL SHEAR STRESS FAILURE

4.1 Simulation of Interfacial Failure using Monte Carlo Simulations

4.1.1 Introduction

The earlier part of the simulations focuses more on the idealized shear specimens which do not exist in reality. There always exist flaws within the specimen at the interface which go unaddressed in the case of 'idealized' simulations. The objective of this part of the thesis is to look at the failure of the shear specimens using a Monte Carlo approach. There is randomness involved in the length and location of flaws along the interface. Though flaws will be present even in the bulk material, we are not interested in these types of flaws as the specimen always fails along the interface. Thus, a Monte Carlo simulation making use of this randomness would provide better insight into the failure strength of shear specimens.

An initial flaw is assumed to present in the interface which causes the final failure and the resulting distribution of shear strengths is examined and compared with the experimental histograms. The initial flaw might be a material defect or could be an air bubble introduced into the interface as a result of bonding. This might be a 'weak' spot at the interface from which the final failure causing crack could originate.

4.1.2 Assumptions

The underlying assumptions in this simulation are acknowledged here. It is assumed that only one initial flaw causes the final failure in the material. This need not be the case in reality where there might be several competing cracks causing ultimate failure. However, for the sake of simplicity, one crack is assumed to cause final failure though it is possible to simulate multiple cracks using the same models described below. Also, a two-dimensional model is used which neglects the presence of cracks through the thickness of the specimen. However, the thickness of the specimen is much lesser compared to its width which justifies the analysis. Again, the flaw size is assumed to take into account most of the representative flaws. In this case we use a probability distribution which accounts for the randomness in the flaw sizes and locations along the interface. Since the actual distribution of flaw sizes is unknown, three different distributions with varying parameters are used in the analysis. Again, the value of K_{IIC} is not known with certainty and hence several values are tried out. As only the ratio between the shear strengths of the two specimens is of importance here, these variations in values can be justified. Finally, a mathematically sharp crack is assumed for the purposes of simulation. This again need not exist in reality, but is assumed for the purposes of simplicity.

4.1.3 Methodology

An initial flaw is assumed to exist in the interface of the shear specimens, which causes final failure. The location of this flaw along the interface and its length is assumed

to vary in a random fashion. The final failure criterion is defined using critical stress intensity factors. This criterion which is adopted from Rammsteiner (1993) is as follows.

$$K_{II} > K_{IIC} = K_{IC} \tag{4.1}$$

The K_{IIC} value is difficult to obtain and is assumed to be close to the K_{IC} value. The value of K_{IC} is taken as 0.38 Mpa $\sqrt{m}$ (Xu and Rosakis, 2003). The specimen is assumed to have failed once the stress intensity factor exceeds the value of the critical stress intensity factor. The loading is increased sequentially until the critical stress intensity value is achieved.

The crack length is initially assumed to vary in a normal fashion and it was assumed that 90% of the samples were covered in the 100-1000 micron range. A 5% probability was assigned to the lower bound of 100 micrometers and a 95% probability was assigned to the upper bound of 1000 micrometers. A histogram of the crack length realizations is shown in Fig. 4.1. The crack position, which was defined by the position of the center of the crack, was however assumed to be a uniformly distributed variable as it equally likely to be found anywhere along the length of the interface. Also, it was assumed that the crack was always inside the interface and did not originate at the edges. This assumption was chosen, as it is highly unlikely for an edge crack to be present in reality. A Monte Carlo simulation was carried out with the crack length and crack size as the two variables and for each simulation the model was built and the boundary conditions applied. The meshing depends on the length and location of the crack. The model is constructed using symmetry of the individual halves. But the loading is anti-symmetric and is applied only after the entire model is generated and not on the individual halves. Loads are applied according to Kumosa et al. after checking for tensile

forces on the loading blocks as discussed earlier. The applied displacement was increased until the specimen 'failed' and then the interfacial shear stress was recorded. The value of the shear stress was taken as the interfacial shear force divided by the area of cross section of the specimen. The shear force in turn was computed by integrating the value of shear stress across the interface over all the nodes. The value of K_{II} was computed as

$$K_{II}=C^{*}\sigma_{xy}\sqrt{\pi a} \tag{4.2}$$

Where σ_{xy} is the shear stress at the crack tip and a is the half crack length. C is a constant whose value is unknown, but in the present case, this value is fitted based on the experimental data for a K_{IIC} value of 0.38 $Mpam^{1/2}$. Since we are only interested on the ratio of the shear strengths of the two types of specimens, the exact value of the constant C is not of much significance here. Since, the analysis has two crack tips (the crack is always an interior crack) the higher of the two K_{II} values is always used in comparison with the K_{IIC} value. This is because the specimen will fail when either of tips reaches the critical K_{II} value. The analysis is repeated for a fixed number of steps with values of crack length and crack location generated from the distribution. The shear strength values from the simulation are stored and a histogram of all the values is plotted. Fig. 4.1 indicates a schematic flow chart of the entire methodology used in this analysis.

In this analysis it should be noted that for failure the requirement that the K_{II} value should exceed the critical one. This is achieved by increasing the value of applied load. Hence, in order to be efficient with the analysis, it is necessary to determine only that load which would cause failure of the model specimen. Treating this problem as an optimization would only add unnecessary computational difficulty which would be undesired in this case. However, the initial value of applied displacement is chosen

sufficiently high in order to allow for faster computation. Also, this value is chosen higher for smaller crack lengths depending on its location. The value of K_{II} is also recorded to double check if the critical value is just exceeded. In case the difference between the values of K_{II} and K_{IIC} is too high, the realization is ignored.

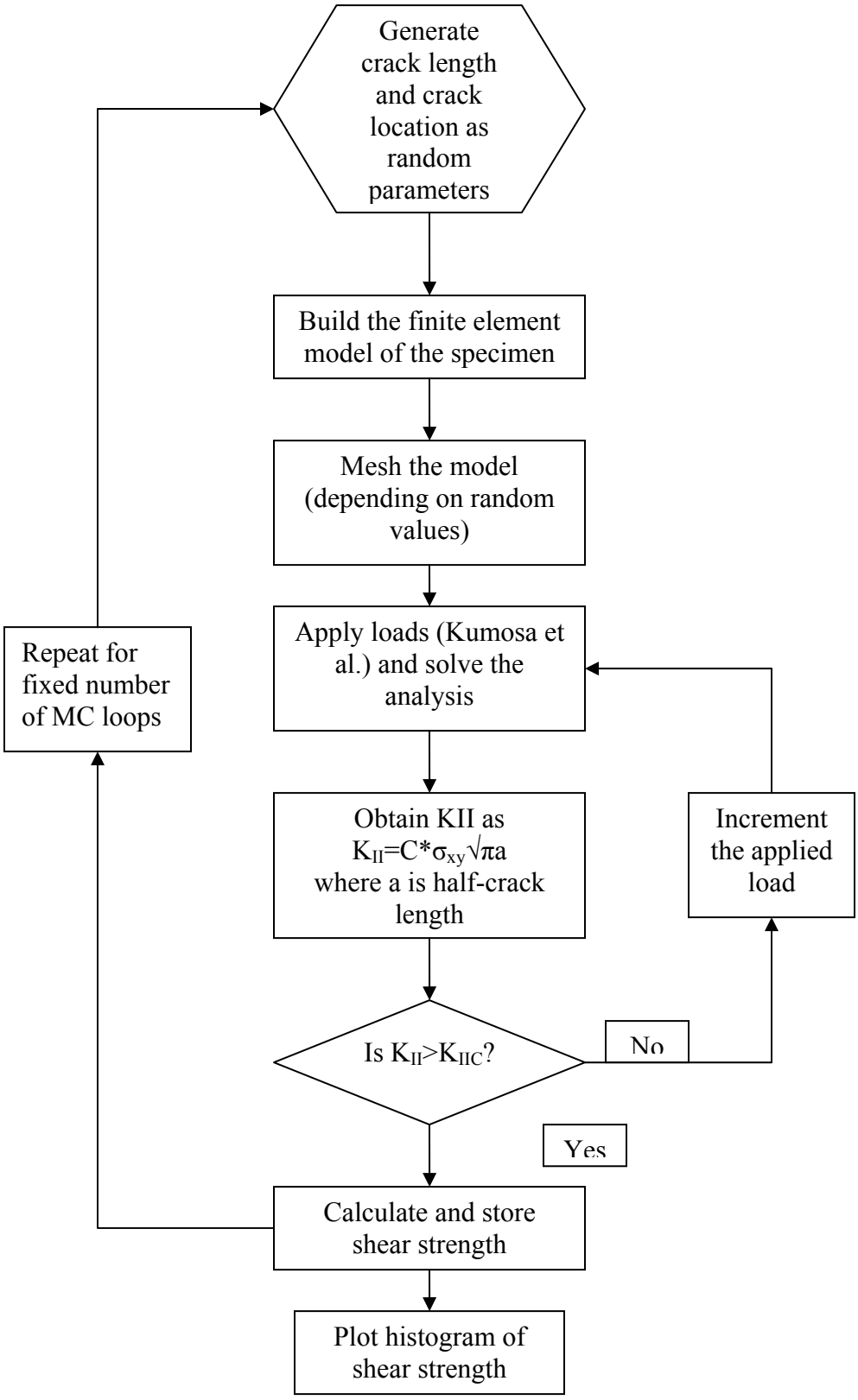

Fig. 4.1 Methodology used for Monte Carlo simulations

4.1.4 Random parameters

Since the value of K_{IIC} is not known accurately, four different values are used in this simulation and the ratio between the shear strengths of the Iosipescu and Butt-shear specimens is compared. The value of the constant is fitted using experimental data for a value of K_{IIC}=0.38 Mpa $m^{1/2}$. Other values of K_{IIC} are chosen as 0.57, 0.76 and 0.95.

In order to study of the effect of different initial crack length distributions, three different types of initial distributions are chosen. A normal distribution truncated at the two extremes of crack sizes is chosen as a standard distribution to facilitate comparison between variations of K_{IIC} and initial crack length distribution. It should be noted here that the initial distributions of crack lengths for Iosipescu and Butt shear specimens would be different as their area of cross sections vary. An Iosipescu specimen has a cross sectional area about 60% lesser than that of its butt shear counterpart. The individual values of cross sectional area vary with the type of material. (Thickness values are different for different materials, but are the same for Iosipescu and butt shear specimen of a single type of material). However, the interfacial length is the same for all types of materials. Hence, for all types of materials the cross sectional area for the Iosipescu specimen is 60% lesser than that of a butt-shear specimen. Therefore, the distribution of crack lengths for these two types of specimens should differ by this amount in the abscissa having the same range of values of crack lengths. When a normal distribution is chosen, the resulting distributions for Iosipescu and Butt shear specimens will be as shown in Fig. 4.2. Since, the two specimens have different interfacial cross sectional areas, the frequency of a flaw occurring in an Iosipescu specimen (having 40% reduced area than the butt-shear specimen) will be reduced by the same amount as the ration of

cross sectional areas. This fact is made use of in generating probability distributions. For a normal distribution, the probability density function or PDF is given as

$$f_x(x)=(\sigma_x\sqrt{2\pi})^{-1} * \exp\left(-0.5*((x-\mu_x)/\sigma_x)^2\right) \quad (4.3)$$

Here σ_x is the standard deviation and μ_x is the mean of the distribution. If the above distribution is taken for a butt-joint shear specimen, the same distribution for a normal distribution would be

$$f_x(x)=0.6 * (\sigma_x\sqrt{2\pi})^{-1} * \exp\left(-0.5*((x-\mu_x)/\sigma_x)^2\right) \quad (4.4)$$

Here, the factor 0.6 is the cross sectional area ratio and accounts for the difference in cross sectional areas of the two specimens. This distribution is again normal with a mean of 1.667 (1/0.6) times the original mean (of the butt-joint specimen distribution) and a standard deviation value of 1.667 times the original standard deviation. The resulting realizations however, have to be multiplied by 0.6 to get the same range of x values. Thus, the resulting distributions for the Iosipescu and Butt-joint shear specimens would look like in Fig. 4.2.

A similar approach is followed for the Weibull distributions, in which the frequency is factored by a value of 0.6 and then the resulting distribution is converted into another Weibull distribution with modified parameters. This is done in order to allow for a fair comparison. The Weibull distribution for PDF is given as

$$f(x;k,\lambda)=(k/\lambda)*(x/\lambda)^{k-1}*\exp(-(x/\lambda)^k) \quad (4.4)$$

where k is the shape parameter and λ is the scale parameter. Again, for an Iosipescu specimen, the frequency of this distribution is factored by a value of 0.6 to account for the cross-sectional area ratio. The resulting distributions from the Weibull graphs are shown in Fig. 4.3 and Fig.4.4.

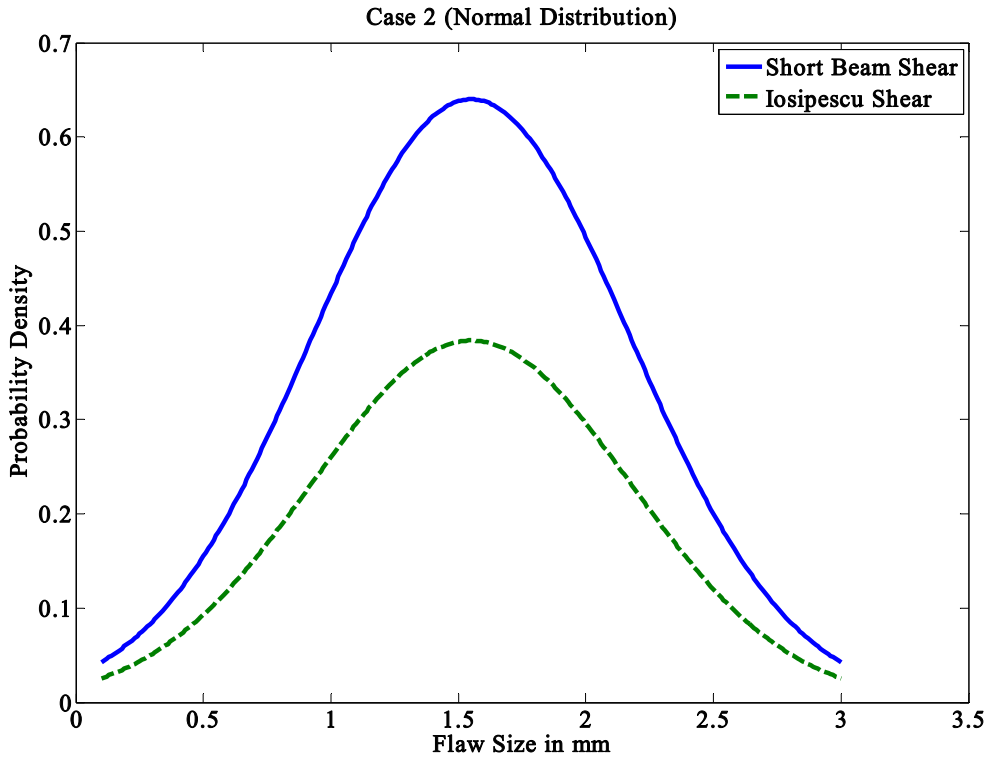

Fig. 4.2 Crack size distribution (Normal) for Iosipescu and Short beam shear specimens

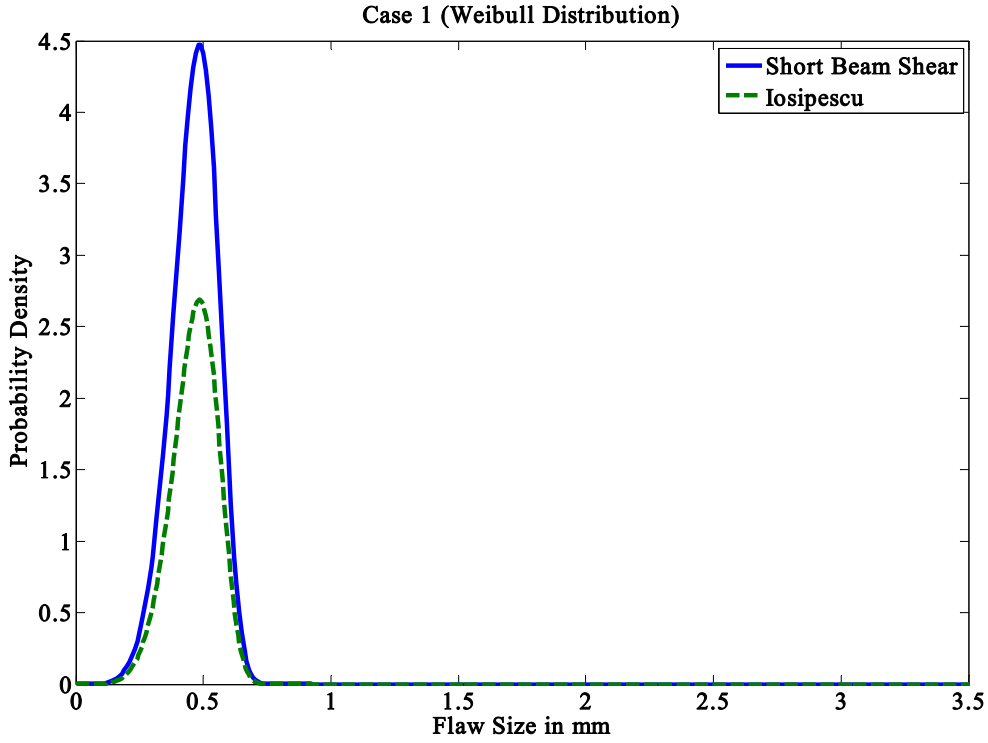

Fig.4.3 Crack size distribution (Weibull) with values skewed towards smaller crack size

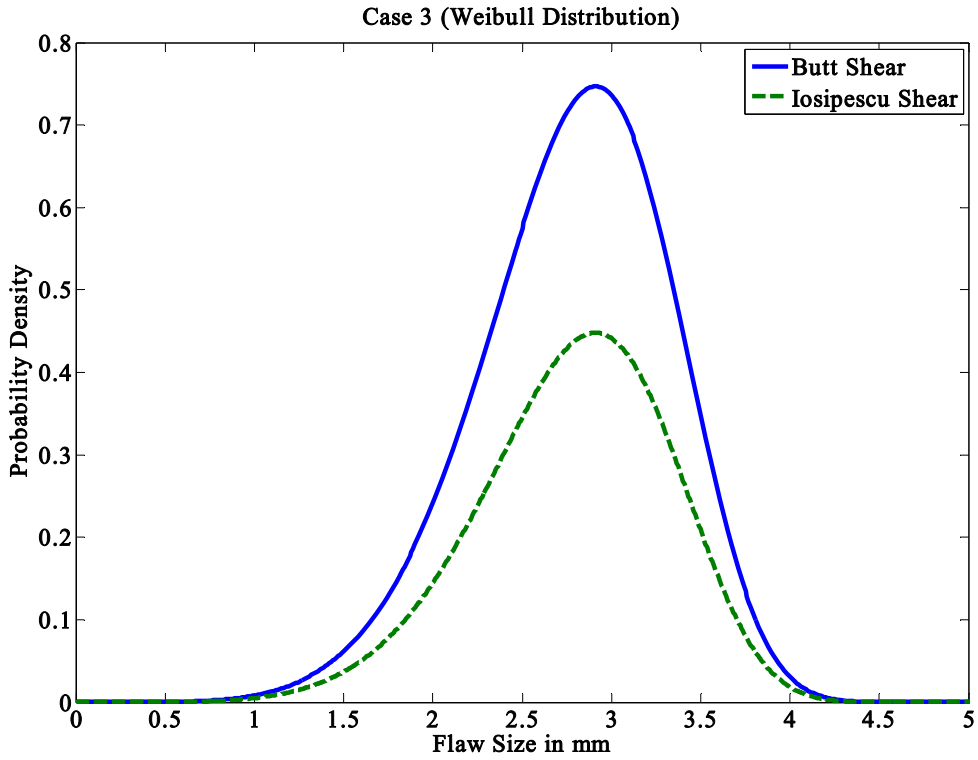

Fig.4.4 Crack size distribution (Weibull) with values skewed towards larger crack size

4.2 Results from the simulations

The above methodology was applied to obtain the output distribution of shear stress values for Iosipescu and Butt shear specimens. Only one type of material was used here, namely polycarbonate. This would however, represent all the three materials satisfactorily as the only difference would be the elastic moduli. Though the shear strengths value may vary, the ratio between the shear strengths would be the same in all three cases. Also, the value of K_{IIC} is not known accurately for Aluminum which would cause error in our simulations. The results of the simulations are presented in Table 4.1. Here the ratio of the mean value of shear strength of the Iosipescu specimen to that of the butt joint shear specimen is presented. It should be noted that the aim here is not to

reproduce the exact experimental values but to compare the ratio with the experimental one. The experimental value of the ratio presented here is 1.291 and it is seen that it is quite close to the simulated values. It is also seen that there is not a large variation when the K_{IIC} value or the type of distribution is varied. The normal distribution with a KIIC value of 0.38 is used as a baseline for comparison purposes. When the crack sizes are skewed towards the larger value the ratio tends to increase.

Table 4.1 Variation of shear strength ratio

K_{IIC}	Type of Specimen	Mean (In Mpa)	Ratio
0.38			
	Iosipescu	8.014	1.065
	Short Beam	7.524	
0.57	Iosipescu	11.123	1.131
	Short Beam	9.831	
0.76	Iosipescu	14.239	1.043
	Short Beam	13.656	
0.95	Iosipescu	18.385	1.035
	Short Beam	17.770	

Weibull Distribution

Case 1	Iosipescu	8.014	1.065
	Short Beam	7.524	
Case 3	Iosipescu	10.400	1.116
	Short Beam	9.317	

CHAPTER V

CONCLUSIONS

Though a lot of literature has been published on the Iosipescu shear test over the past few decades, no one has studied the necessity of this shear test. The shear test though seemingly ideal for one of its kind is complicated, requires increased cost and skill, and needs greater time and patience in comparison to other simple tests. The value of interest here is shear strength, which is a basic material property much like the Elastic moduli or Poisson's ratio. The Iosipescu shear test gives a fairly accurate value of interfacial strength as is seen from our experimental comparison, but is more complicated and time consuming.

In this thesis experimental and numerical means have been used to demonstrate the redundancy involved in using Iosipescu and butt-joint shear specimens. Both the specimens give a value of shear which is quite close. The only difference would be in their respective variations. This occurs due to the presence of uniformity of shear across the interface of the Iosipescu specimen which is absent in case of a butt-joint specimen. The Photoelastic fringe patterns help understand the development of shear at the interface and serve to validate the finite element model. Finally, the Monte Carlo simulations provide insight into the failure process at the interface. The simulations agree well with our experimental data.

REFERENCES

1. Bansal A, Kumosa M. Analysis of Double Edge-Cracked Iosipescu Specimens under Biaxial Loads, *Eng Fract Mech* 1998; 59: 89.

2. Barnes JA, Kumosa M, Hull D, Theoretical and experimental evaluation of the Iosipescu shear test, *Comp. Sci. and Tech.* 28, pp. 251-268, 1987.

3. Bogy DB, Two edge-bonded elastic wedges of different materials and wedge angles under surface tractions, *J. of App. Mech.* 38 pp**.** 377-386, 1971.

4. Chan A., Chiu WK., Liu XL. Determining the elastic interlaminar shear modulus of composite laminates. *Composite Structures* 2007;80(3); 396-408

5. Chiang YMM, Jianmei H. An analytical assessment of using the Iosipescu shear test for hybrid composites. *Composites: Part B* 2002;33:461

6. D'Almeida JRM, Monteiro SN. The Iosipescu Test Method as a Method to Evaluate the Tensile Strength of Brittle Materials, *Polymer Testing* 1999; 18: 407.

7. Ding S., Erdinc I., Buchholz FG, Kumosa M. Optimization of the adhesive joint Iosipescu specimen for pure shear test. *Intl. J of Frac.* 1996;76;1-20

8. El-Hajjar R, Haj-Ali R. In-plane shear testing of thick-section pultruded FRP composites using a modified Arcan fixture. *Composites: Part B* 2005;35;421-428

9. Grediac M, Pierron F, Vautrin A, The Iosipescu in-plane shear test applied to composites: A new approach based on displacement field processing, *Comp. Sci. and Tech.* 51, pp. 409-417, 1994.

10. Hawong Jai-Sug, Shin Dong-Shul, Baek Un-Cheol, Validation of pure shear test device using finite element method and experimental methods, *Engg. Frac. Mech.* 71 pp. 233-243, 2004.

11. Ho H, Tsai MY, Morton J, Farley GL, Numerical analysis of the Iosipescu specimen for composite materials, *Comp. Sci. and Tech.* 46, pp. 115-128, 1993.

12. Kumosa M, Han Y, Non-linear finite analysis of Iosipescu specimens, *Comp. Sci. and Tech.* 59, pp. 561-573, 1999.

13. Kwon HJ., Jar PYB. Fracture toughness of polymers in shear mode. *Polymers* 2005;46;12480-12492

14. Li J., Zhang X. Crack initiation prediction for V-notches under mixed-mode loading in brittle materials. *J of Mechanics of materials and structures* 2006;1;1385-1404

15. Melin NL, Neumister JM. Measuring constitutive shear behavior of orthotropic composites and evaluation in the modified Iosipescu test. *Composite Structure* 2006;76:106

16. Ramsteiner, F. (1993) An approach towards understanding mode II failure of poly (methyl methacrylate). *Polymer*, **34**, 312-317.

17. Sengupta S. PhD Thesis, Interfacial Design and Mechanics analysis of advanced materials and structures, Vanderbilt University, 2007

18. Sullivan JL. The Use of Iosipescu Specimens, *Exp Mech* 1987:326.

19. Sullivan JL, Kao BG, Van Oene H. Shear Properties and a Stress Analysis Obtained from Vinyl-Ester Iosipescu Specimens,I 1984: 223.

20. Sukumar N, Kumosa M. Finite Element Analysis of Axial Splits in Composite Iosipescu Specimens, *Int J Fract* 1993; 62: 55.

21. Walrath DE, Adams DF. The Iosipescu Shear Test as Applied to Composite Materials, *Exp Mech* 1982: 105.

22. Xavier JC, Garrido NM, Oliviera M, Morais JL, Camanho PP, Pierron F. A comparison between the Iosipescu and off-axis shear test methods for characterization of Pinus Pinaster Ait, *Composites Part A* 35 pp. 827-840, 2004.

23. Xu, L.R., Huang, Y.Y. and Rosakis, A.J. Dynamic crack deflection and penetration at interfaces in homogenous materials: Experimental studies and model predictions, *Journal of the Mechanics and Physics of solids,* 2003, 51, 461-486.

24. Xu, L.R. and Rosakis, A.J. (2002) Impact failure characteristics in sandwich structures; Part II: effects of impact speed and interfacial strength. *International Journal of Solids and Structures*, **39**, 4237-4248.

25. Xu LR, Sengupta S, Kuai H, An experimental and numerical investigation of adhesive bonding strengths of polymer materials, *Intl. J. of Adhesion and Adhesives* 24, pp. 455-460, 2004a.

26. Xu, L.R., Kuai, H. and Sengupta, S. (2004b) Dissimilar Material Joints with and without Free-edge Stress Singularities, Part I. A Biologically Inspired Design. *Experimental Mechanics*, **44**, 608-615.

27. Xu L.R., Sengupta, S. and Kuai, H. (2004c) Dissimilar Material Joints With and Without Free-Edge Stress Singularities: Part II. An Integrated Numerical Analysis. *Experimental Mechanics*, **44**, 616-621.